Co-W Bimetallic Carbides as Sulfur Host for High-Performance Lithium–Sulfur Batteries

Dongke Zhang
Nanchang University
Ting Huang
Nanchang University
Pengfei Zhao
Nanchang University
Ze Zhang
Nanchang University
Xingtao Qi
Nanchang University
Zhenyu Yang
Nanchang University
Jianxin Cai (cjx@ncu.edu.cn)
Nanchang University https://orcid.org/0000-0003-4382-095X

Research Article

Keywords: Co3W3C, Synergy, Shuttle effect, Block structure, Lithium-sulfur batteries

DOI: https://doi.org/10.21203/rs.3.rs-308410/v1

Abstract

Due to the low conductivity of sulfur and the dissolution of polysulfides, the research and application of lithium-sulfur (Li-S) batteries have encountered certain resistance. Increasing conductivity and introducing polarity into the sulfur host can effectively overcome these long-standing problems. Herein, We first prepared Co_3W_3C@ C@ CNTs / S material and used it in the cathode of lithium-sulfur batteries, The existence of carboxylated CNTs can form a conductive network, accelerate the transmission of electrons and improve the rate performance, and polar Co_3W_3C can form a strong interaction with polysulfide intermediates, effectively inhibiting its shuttle effect, improving the utilization of sulfur cathode electrodes, and improving the capacity and cycle stability. The Co_3W_3C@C@CNTs / S electrode material has a capacity of 1,093 mA h g-1 at a 0.1 A g^{-1} and 482 mA h g-1 at 5 A g^{-1}. Even after 500 cycles of 2 A g^{-1}, the capacity of each cycle is only reduced by 0.08%. The excellent stability of this material can provide a new idea for the future development of lithium-sulfur batteries.

Introduction

Nowadays, considering the increasing demand for portable power supply, the application of electrochemical energy storage devices has been widely developed [1, 2, 3].Traditional lithium-ion batteries (LIB) based on plug-in electrodes are close to their energy density limits, making it difficult to meet the rapidly increasing demand for electric vehicles and portable electronic devices[4, 5]. Therefore, rechargeable batteries and supercapacitors have become popular and have been further explored. For rechargeable lithium-sulfur (Li-S) batteries, due to their high energy density (2,600 Wh kg^{-1}) and large theoretical specific capacity (1,675 mA h g^{-1}), they increasingly meet the needs of human development [6] .People think this is the next generation of promising electrochemical energy storage devices. However, the commercialization of Li-S batteries faces many problems. For example,1) lithium polysulfur compounds are dissolved in the electrolyte; 2)Sulfur has poor conductivity; 3) The volume expansion of sulfur during charging and discharging may cause battery damage [7, 8, 9].

The above problems achieve high conductivity and long cycle stability by combining sulfur with other material encapsulation.Among various carrier materials, carbon materials are widely introduced as host in LSBs [10]. Such as Porous carbon [11], graphene [12, 13], carbon nanotubes (CNTs) [14, 15], hollow carbon nanofibers/nanospheres [16–18]. These carbon-based nanocomposites show excellent specific capacity compared with pure sulfur cathodes in the initial cycles. However, considering the limited capacity of non-polar carbon substrates to encapsulate polar polysulfide, the capacity will decline rapidly in the following cycles [19, 20]. The main role of carbon materials in the immobilization of polysulfides is physical absorption rather than chemical interaction[21]. Therefore, chemical absorption between polar matrix and polar polysulfide is the focus of future research. Conductive polymers [22], MXene [23], nitride [24], and hydroxide [25] have been used as host materials for lithium-sulfur batteries [26, 27]. These materials show good electrochemical performance and inhibit the shuttle effect to some extent [28]. Transition metal carbides (e.g., TiC, WC, and NbC) [29] are used in Li–S batteries because of their unique

metal properties, such as high conductivity (10^4 S cm^{-1}).The above materials can not only improve the conductivity of the sulfur anode, but also can effectively inhibit the blocking of polysulfides through strong bond cooperation.

The excellent performance of W_2C and Co in Li–S batteries serves as basis for the combination of W_2C and Co to prepare bimetallic carbides.[30, 31]. Herein, we prepared Co_3W_3C@C@CNTs/S by using $Co(NO_3)_2{\cdot}6H_2O$,$(NH_4)_{10}H_2(W_2O_7)_6$, $C_2H_4N_4$, CNTs and elemental sulfur through a simple one-step pyrolysis and melt diffusion method. The Co_3W_3C was used as a battery material for the first time, and these materials have shown good chemical performance. The Co_3W_3C@C@CNTs/S electrode exhibited a capacity of 1,093 mAh g^{-1} at 0.1 A g^{-1} and 482 mAh g^{-1} at 5A g^{-1}. Even after 500 cycles of 2 A g^{-1}, the capacity of each cycle is only reduced by 0.08% each cycle.

Experimental Section

Synthesis of carboxylated carbon nanotubes

To effectively disperse homogeneous carbon nanotubes in water, we carboxylated the original carbon nanotubes before usage. First, ultrasonic dispersion of the original CNTs (XiLong Scientific) was carried out in deionized (DI) water followed by agitation of 30% H_2O_2 for 5 h. After washing and drying, the CNTs obtained were dispersed in nitric acid solution, refluxed for 5 h at 100 ℃, washed to neutral, and dried at 80 ℃ for later use.

Synthesis of the Co_3W_3C@C@CNTs/S, Co_3W_3C@C/S, and CNTs/S Composite

Typically, 0.84 mmol of cobalt nitrate hexahydrate ($Co(NO_3)_2{\cdot}6H_2O$, Aladdin), 0.07 mmol of ammonium tungstate hexahydrate ($(NH_4)_6W_7O_{24}6H_2O$, Aladdin), 1 g of dichrodicylamine ($C_2H_4N_4$, Aladdin), and an appropriate amount of carboxylated CNTs were dispersed in 40 mL of DI water. continuously stirred and dried at 60 ℃ for 10 h and placed in a tubular furnace under N_2 flow at 800°C for 2 h. The heating rate was controlled at 5°C min^{-1}. Subsequently, Co_3W_3C@C@CNT composites (without CNTs) were obtained. Then, Co_3W_3C@C@CNTs and sulfur powders (95% purity, Aladdin) were milled and mixed evenly at a mass ratio of 1:4. The mixture obtained by grinding was placed in a reaction kettle filled with inert protective gas, and the Co_3W_3C@C@CNTs/S composite was prepared by a simple fusion–diffusion method (155 ℃, 12 h). CNTs/S and Co_3W_3C@C/S composites were also obtained.

Material Characterizations

The samples were characterized by XRD with a Bruker D8 diffractometer, the 2θ was 10–80°, and the tube pressure and tube flow were 40 kV and 30 mA, respectively. Use Quanta 200FEG and JEM-2100 electron microscopes to observe the morphology, crystal structure, element composition and distribution of samples.Use TGA/DSC 3 + differential thermal and thermogravimetric analyzer to test samples within the range of 30–800℃,10℃min^{-1} to weight loss behavior. ESCALAB250XI X-ray energy spectrometer was used to characterize the element composition and valence state of the sample surface. we

performed BET measurements on a 3H-2000PS1 Surface Area and Porosimetry Instrument to characterize the specific surface area and pore size .Use XploRA PLUS Raman spectrometer to perform Raman test on the sample, and the test laser wavelength is 633 nm.

Electrochemical measurements

Take appropriate amount of CNTs/S, Co_3W_3C@C/S and Co_3W_3C@C@CNTs/S composite materials and Super P, PVDF according to the mass ratio of 7:2:1, add appropriate amount of NMP as solvent, stir and mix evenly. The obtained slurry was uniformly coated on aluminum foil, and after being completely dried, it was punched into a disc with a diameter of 12 mm, and the sulfur loading was 1.2–1.5 mg cm^{-2}. Take CNTs/S, Co_3W_3C@C/S and Co_3W_3C@C@CNTs/S composite materials as the cathode electrode, lithium sheet as the anode electrode, Celgard 2300 as the separator, LiTFSI (1.0 M) and $LiNO_3$ (0.2 M),and DOL/DME (1:1, *v/v*) The solution is electrolyte and assembled into 2025 button cell in an argon glove box. PARSTAT 2273 and CHI-660B electrochemical workstation are used to conduct ESI and CV tests on the battery, and Xinwei battery test system is used to test the cycle performance of the battery.

Lithium polysulfide adsorption study

To intuitively understand the chemical adsorption capacity of materials to polysulfide lithium, we used the CNT, Co_3W_3C@C, and Co_3W_3C@C@CNT composites as adsorbents for the Li_2S_8 adsorption experiment. First, weigh a certain amount of lithium sulfide and sulfur element in a stoichiometric ratio (1:7) and dissolve it in DOL/DME (*v/v* = 1: 1) to prepare a 5 mM Li_2S_8 solution. Take 5 mL Li_2S_8 solution and add 5 mg CNTs, Co_3W_3C@C and Co_3W_3C@C@CNTs samples respectively, and observe the color change of the solution over time.

Results And Discussion

The Co_3W_3C@C@CNTs/S was via a simple one-step pyrolysis and melt diffusion method, as clearly seen in Fig. 1 .And detailed morphology was obtained by SEM and TEM. Figure 2a–b show that Co_3W_3C@C@CNTs are irregular block materials with rough surface. Based on the elemental distribution map (Fig. 2c), Co, W, and C are uniformly distributed in the material. When sulfur was loaded, the rough surface of Co_3W_3C@C@CNTs became relatively smooth (Fig. 2d–e). This finding indicates that sulfur is not only loaded into the pores of Co_3W_3@C@CNTs materials, but also exist on the surface of materials.Besides, according to the elemental distribution map (Fig. 2f), sulfur was uniformly distributed in the Co_3W_3C@C@CNT composites, thus illustrating the successful preparation of Co_3W_3C@C@CNTs/S.

Figure3 shows the TEM diagram of Co_3W_3C@C@CNTs composite material. The figure shows that the particle size of Co_3W_3C particles is 5–30 nm (Fig. 3a–c) and is uniformly distributed in carbon blocks, indicating that the presence of carbon matrix can inhibit the agglomeration of Co_3W_3C nanoparticles and improve the utilization ratio of Co_3W_3C. CNTs can connect Co_3W_3C@C to form a conductive network and accelerate the electron transfer rate in the material [32]. Many micropores are distributed on each slice.

The TEM (HRTEM, Fig. 3d) demonstrates the lattice spacings of 0.63 and 0.34 nm, belonging to the crystal surface of Co_3W_3C (111) and graphite carbon (002), respectively [33].

The XRD patterns of Co_3W_3C@C@CNTs (Fig. 4a) and Co_3W_3C@C@CNTs/S **(FigureS1)** indicate that Co_3W_3C has a good crystal structure. Figure 4a shows that in the composite material, Co_3W_3C has a crystalline structure, and its characteristic diffraction peak is compounded with JCPDS NO. 27-1125 standard card phase [34]. In addition, according to the relative strength of carbon (24°) and Co_3W_3C characteristic peaks, Co_3W_3C@C@CNT composites were successfully prepared through a simple one-step thermal decomposition method. **Figure S1** explain that sulfur in the composite material has a distinct crystal structure, and its characteristic diffraction peak is compounded with JCPDS NO. 08-0247 standard card phase[35]. In the composite materials with high sulfur content, sulfur content is easy to deposit and adhere to the surface of the carrier material, thus showing strong XRD characteristic peak, and even masking the characteristic diffraction peak of the carrier material.

Figure4b describes the Raman spectrum of CNTs, Co_3W_3C@C, and Co_3W_3C@C@CNTs composites. The D peak (1,338 cm^{-1}) and G peak (1,572 cm^{-1}) peculiar to carbon materials appeared in the Raman spectra of the three samples. The ID/IG ratio represents the degree of graphitization of carbon. The ID/IG ratios of CNT, Co_3W_3C@C, and Co_3W_3@C@CNT composites are 0.32, 1, and 0.9, respectively. This finding description that added highly graphitized CNTs can improve the graphitization degree of Co_3W_3C@C@CNT composites,significantly improve the conductivity of composite materials, cathode sulfur utilization rate and lithium-sulfur battery performance to a certain extent[36, 37].In Fig. 4c, we can see that Co_3W_3C@C@ CNTs shows a typical type I isotherm. In relatively low pressure areas, gas adsorption increases very rapidly.The specific surface area and pore volume ratios of Co_3W_3C@C@CNTs were 132.25 $m^2\ g^{-1}$ and 0.1595 $cm^3\ g^{-1}$, and the pore diameter distribution was mainly concentrated at 4 nm. When sulfur was loaded, Co_3W_3C@C@CNTs/S were reduced to 28.43 $m^2\ g^{-1}$ and 0.0412 $cm^3\ g^{-1}$, respectively. **Figure S2** shows the TG curve of Co_3W_3C@C@CNT composite material in air atmosphere of 30–800 ℃. The mass loss below 200 ℃ was caused by the steaming of crystal water adsorbed on the surface of the material, and the relatively gentle weight loss at 400–600 ℃ was caused by the oxidation of partial carbon and all Co_3W_3C to generate CO_2 and $CoWO_4$. The rapid weight loss between 600 ℃ and 700 ℃ was caused by the total oxidation of the remaining carbon. Results showed that the content of C in the Co_3W_3C@C@CNT composite was 50 wt%.In order to determine the S content in the composite material, the sample was subjected to TGA test under a nitrogen atmosphere in Fig. 4d, at 200–300℃, elemental sulfur is heated and vaporized, and the quality of the sample drops sharply. The thermal weight loss curve shows that the S content in the Co_3W_3C@C@CNTs sample is about 80 wt%.

The electronic state, chemical state, and element composition of Co_3W_3C@C@CNTs were studied by XPS. In **Fig. 5a**, the peak at 781.9 eV, 532.8, 285.9 and 35.8 eV are ascribed to Co 2p, O 1s, C 1s and W 4f, respectively. Figure 5b can be seen that the Co 2p orbital is split into Co $2p_{3/2}$ and Co $2p_{1/2}$,located at 782.0, 797.5 eV, respectively.And S1 and S2 exist at 784.9 and 803.8 eV, because of the presence of Co^{2+}

[38]. In addition ,Co^0 at 778.8 eV Verifies the existence of Co–W bimetallic carbide. W 4f signals in Co_3W_3C@C@CNTs at 31.6 and 33.8 eV are corresponds to W $4f_{7/2}$ and W $4f_{5/2}$, these indicate the presence of WC bonding(**Fig. 5c**)[39, 40].Lastly, C 1s was observed at 284.6 eV, indicating the existence of sp2 bonded carbon. **(Fig. 5d)**.

In order to explore the feasibility of Co_3W_3C@C@CNTs/S composite material as Li-S battery cathode. Figure 6a shows the CV diagrams of CNTs/S, Co_3W_3C@C/S, and Co_3W_3C@C@CNTs/S at 0.1 mVs^{-1} with the voltage range of 1.7 to 2.8 V. It also shows that all the three composite positive electrodes have two reduction peaks, and one oxidation peak [41]. The first reduction peak (~ 2.5 V) corresponding to the conversion of S_8 to order long-chain polysulfides, such as Li_2S_4, Li_2S_5, Li_2S_6, Li_2S_7, and Li_2S_8 [42]. The second reduction peak at approximately (2.1 V) represents the gradual reduction of long-chain polysulfide to insoluble Li_2S_2 and Li_2S. In comparison with CNTs/S, the Co_3W_3C@C/S and Co_3W_3C@C@CNTs/S composites have higher peak current, indicating that the presence of Co_3W_3C@C is conducive to the transformation of polysulfide. The first discharge capacities**(FigureS3a)** of CNTs/S,Co_3W_3C@C/S,and Co_3W_3C@C@CNTs/S were 983, 1,040, and 1,093 mA h g^{-1}, respectively. Besides, Multiplier and cycle performance are also important parameters for Li–S batteries. Figure 6.**b** shows that the cathode of Co_3W_3C@C@CNTs/S has a good multiplier performance, the discharge specific capacity is 1,093 mA h g^{-1} at 0.1 A g^{-1}. When the current density increased to 5 A g^{-1}, its capacity remained much higher by 482 mA h g^{-1} than the cathode electrode of CNTs/S. **Figure S3b** shows the charge and discharge curves of each electrode at 5 A g^{-1}. Even at 5 A g^{-1}, the cathode of Co_3W_3C@C/S and Co_3W_3C@C@CNTs/S maintained two obvious discharge platforms. The cathode of Co_3W_3C@C@CNTs/S has good multiplier performance, because the presence of Co_3W_3C can accelerate the reaction kinetics of polysulfide transformation. In comparison with CNTs/S and $Co_3W_3C_3$@C/S, the cathode of Co_3W_3C@C@CNTs /S showed better long cycle performance **(**Figs. 6c–d**).** The capacity was maintained at 531 mAh g^{-1} after 200 cycles at 0.2 A g^{-1}, and the capacity attenuation rate was 0.18%/time. Even at 2 A g^{-1}, the capacity of the first discharge was 688 mAh g^{-1}, and the capacity remained at 407 mAh g^{-1} after 500 cycles. The capacity attenuation rate was only 0.08%/time, indicating that the carrier material of Co_3W_3C@C@CNTs could effectively inhibit the circulation effect of polyretention and improve the cycling stability of Li–S batteries. In addition, the Co_3W_3C@C@CNT electrode can exhibit excellent electrochemical performance even under high S loading conditions of approximately 3.8 mg cm^{-2} (**FigureS5a**). Therefore, the Co_3W_3C@C@CNT electrode even at high sulfur content also has excellent performance.

To further explore the effect of chemical interactions between CNTs, Co_3W_3C@C, and Co_3W_3C@C@CNTs on the redox reaction between sulfur and polysulfides, we assembled symmetrical cells for CV and ESI test. As shown in **FigureS4a**,Use two identical graphite electrodes loaded with Co_3W_3C@C and Co_3W_3C@C@CNT and CNTs in Li_2S_8 to assemble a symmetrical cells. It can be seen that the current intensity of the Co_3W_3C@C@CNT electrode is higher than that of Co_3W_3C@C and CNT. It shows that Co_3W_3C@C@CNTs cathode materials, The chemical interaction with polysulfides can effectively

immobilize polysulfides, accelerate the rapid transfer of electrons at the battery interface to improve the redox reaction rate of polysulfides. In addition, the EIS results of symmetrical battery (**FigureS4b**) show that the Co_3W_3C@C@CNT electrode has a small charge transfer resistance, indicating that Co_3W_3C@C@CNTs can accelerate the reaction kinetics of polysulfide conversion[43, 44].

To study the adsorption capacity of CNTs, Co_3W_3C@C, and Co_3W_3C@C@CNTs, we made a comparison and added the material into polysulfide solution. After adsorption after 6 h, the solution containing Co_3W_3C@C@CNTs and Co_3W_3C@C, as shown in **Fig. 7b**, became clearer than the other solutions, while the solution with CNTs showed no obvious color change compared with the blank solution. This indicates that Co_3W_3C@C and Co3W3C@C@CNTs have strong polar-polar adsorption between Li_2S_8, which can effectively adsorb and immobilize polysulfides .UV visible absorption spectrum tests can be seen in **FigureS5b**. After adding Co_3W_3C@C@CNTs, the polysulfide (S_8^{2-}) was significantly reduced, This illustrates the strong adsorption capacity of Co_3W_3C@C@ CNTs for polysulfides from the side [45].After cycling 100 times at 2 A g^{-1}, we obtained images of lithium and separator with CNTs/S, Co_3W_3C@C/S and Co_3W_3C@C@CNTs/S as cathodes, respectively. (**FigureS6**). The images indicate that when Co_3W_3C@C@CNTs/S as cathode,The morphological changes of both are relatively small. Figure 7c shows that CNTs/S, Co_3W_3C@C/S, and Co_3W_3C@C@CNTs/S have charge transfer resistance values of 120,100, and 72 Ω, respectively, indicating that the Co_3W_3C@C@CNTs/S cathode has faster reaction kinetics [46, 47] and can fully play the advantages of high active substance sulfur capacity[48]. Figure 7d proves that Co_3W_3C@C@CNTs/S cathode has a smaller charge transfer resistance, and further shows that Co_3W_3C@C can accelerate the reaction kinetics of polysulfide conversion[50].

We use a schematic diagram to clearly explain the reason why Co_3W_3C@C @CNTs/S is used as a battery cathode material**(**Fig. 8**)**. Firstly, carbon nanotubes acts as the electronic highway. CNTs can improve the conductivity of materials to a certain extent.Secondly, the redox reaction of bimetallic carbide has excellent electronic conductivity [50]Thirdly,Polar Co_3W_3C can form a strong interaction with polysulfide intermediates, effectively inhibiting its shuttle effect, improving the utilization of sulfur cathode electrodes .

Conclusion

In summary, we have successfully prepared Co_3W_3C@C@CNTs composite through a facile one-step pyrolysis method, and Co_3W_3C@C@CNTs/S composites with 80% sulfur content were further prepared by melting–diffusion. The experimental results show that the Co_3W_3C@C@CNTs/S composite material exhibits excellent electrochemical performance when used as the cathode electrode of Li-S battery.Co_3W_3C@C@CNTs/S electrode has high initial capacity and good rate performance (a capacity of 1093 mA h g^{-1} at 0.1 A g^{-1} and 482 mA h g^{-1} at 5 A g^{-1}). The electrode material has good cycle stability. The Co_3W_3C@C@CNTs/S electrode delivers a high reversible capacity of 407 mA h g^{-1} after 500 cycles at 2 A g^{-1}. The capacity only decayed by 0.08% per cycle. The good electrochemical properties of

Co_3W_3C@C@CNTs are mainly attributed to the synergistic effect of Co_3W_3C and CNTs. This provides a new idea for the application of bimetallic carbides in lithium-sulfur batteries.

Declarations

Acknowledgement

This work is financially supported by the National Natural Science Foundation of China (Grant No. 51662029 and 21363015).

Compliance with ethical standards

Conflict of interest

The author declares that there is no conflict of interest when submitting the manuscript, And this manuscript has been approved for publication by all authors.

References

[1]L. Wen, F. Li, H. M. Cheng, Carbon nanotubes and graphene for flexible electrochemical energy storage: from materials to devices. Adv Mater 28,4306-4337(2016).

[2] Z.B. Xiao，Z.L. Li ,X.P. Meng, R.H.Wang, MXene-engineered lithium-sulfur batteries.***J. Mater. Chem. A*** **7**,22730-22743(2019)

[3]B. Liu, J.G. Zhang,W. Xu, Advancing lithium metal batteries. Joule 2,833-845 (2018)

[4]G.R. Li, Z.W. Chen, J. Lu, Lithium-Sulfur Batteries for Commercial Applications.Chem. 4,3-7 (2018)

[5]X.Y. Zhang, H.Y. Zhou, J.G. Wang, Nitrogen-rich microporous carbon framework as an efficient polysulfide host for lithium-sulfur batteries. J .Mater. Sci. 56,3364-3374(2021)

[6] F. Xu,S. Yang,G. Jiang,Q.Ye,B. Wei,H. Wang, Fluorinated, sulfur-rich, covalent triazine frameworks for enhanced confinement of polysulfides in lithium-sulfur batteries, ACS Appl. Mater. Interfaces 9, 37731–37738(2017)

[7]F. Wu, L.L. Shi, D.B. Mu,H.L. Xu ,B.R. Wu, A hierarchical carbon fiber/sulfur composite as cathode material for Li–S batteries.Carbon.86,146-155(2015)

[8]G.S. Jiang,F. Xu,S.H. Yang, J.P. Wu, B.Q. Wei, H.Q.Wang ,Mesoporous, conductive molybdenum nitride as efficient sulfur hosts for high-performance lithium-sulfur batteries.Journal of Power Sources.395,77-84(2018)

[9]X.X.Gu,C.Lai,One dimensional nanostructures contribute better Li–S and Li–Se batteries:Progress, challenges and perspectives, Energy Storage Materials.23,190-224(2019)

[10]Y.X. Yin,S. Xin,Y.G. Guo,L.J.Wan,Lithium–Sulfur Batteries: Electrochemistry, Materials, and Prospects,Angew. Chem. 52,13186–13200（2013)

[11]R.Fang,S.Zhao,P.Hou,M.Cheng,S.Wang,H.M.Cheng,C.Liu,F.Li, 3D Interconnected Electrode Materials with Ultrahigh Areal Sulfur Loading for Li–S Batteries,Adv. Mater 28,3374-3382 (2016)

[12] T.Hu, X.Sun, H.Sun, M.Sun, F.Lu,C.Liu, J.Lian, Flexible free-standing graphene–TiO_2 hybrid paper for use as lithium ion battery anode materials .Carbon 51,322-326 (2013)

[13] M. Yu,R. Li,M. Wu, G. Shi , Graphene materials for lithium–sulfur batteries. Energy Storage Mater. 1,51-73 (2015)

[14] Z.Zhang,H.K. Jing,S. Liu,G.R. Li,X.P. Gao,Encapsulating sulfur into a hybrid porous carbon/CNT substrate as a cathode for lithium-sulfur batteries.J. Mater. Chem. A 3,6827–6834(2015)

[15] J.S. Lee,A. Manthiram,Hydroxylated N-doped carbon nanotube-sulfur composites as cathodes for high-performance lithium-sulfur batteries. J. Power Sources. 343,54-59(2017)

[16] L.Ji,M.Rao,S.Aloni,L.Wang,E.J.Cairns,Y.G.Zhang,Porous carbon nanofiber–sulfur composite electrodes for lithium/sulfur cells.Energy Environ. Sci.4,5053-5059 (2011)

[17]B.K.Cao, Y.Chen, D.Li ,L.H.Yin ,Y.Mo, Synthesis of TiC Nanoparticles Anchored on Hollow Carbon Nanospheres for Enhanced Polysulfide Adsorption in Li-S Batteries.9,3338-3344(2016)

[18]S.S. Li, B.Jin, X.J.Zhai ,H.Li, Q.Jiang, Review of Carbon Materials for Lithium-Sulfur Batteries.3,2245-2260 (2018)

[19]Z.Li, J.Zhang, X.W.Lou,Hollow Carbon Nanofibers Filled with MnO_2 Nanosheets as Efficient Sulfur Hosts for Lithium–Sulfur Batteries. Angew. Chem. 54,12886-12890(2015)

[20]C.X.Li,Z.C.Xi,D.X.Guo,X.J.Chen,L.W.Yin,Chemical Immobilization Effect on Lithium Polysulfides for Lithium–Sulfur Batteries, Small 14,1701986（2017）

[21] C.J.Hu, H.W.Chen, Y.B.Shen, D.Lu, Y.F. Zhao,A.H. Lu , X.D.Wu, W.Lu, L.W.Chen, In situ wrapping of the cathode material in lithium-sulfur batteries, Nat.Commun 8 ,479(2017)

[22]L.L.Yan,D.M.Han,M.Xiao, S.Ren,Y.N.Li , S.J.Wang, Y.Z.Meng,Instantaneous carbonizationof an acetylenic polymer into highly conductive graphene-like carbon and its application in lithium–sulfur batteries.J. Mater. Chem. A.5,7015-7025 (2017)

[24]Z.Cui, C.Zu, W.Zhou, A .Manthiram , J.B.Goodenough,Mesoporous Titanium Nitride-Enabled Highly Stable Lithium-Sulfur Batteries.Adv. Mater 28,6926-6931(2016)

[25] H.K.Jing, L.L.Kong, S.Liu, G.R.Li, X.P.Gao, Protected lithium anode with porous Al_2O_3 layer for lithium–sulfur battery.J. Mater. Chem. A. 3,12213-12219.

[26] J.Liu, L.Yuan, K.Yuan, Z.Li , Z .Hao, J.Xiang, Y.Huang,SnO_2 as a high-efficiency polysulfide trap in lithium–sulfur batteries.Nanoscale 8,13638 -13645(2016)

[27] Z. Li, J. Zhang, B. Guan, D. Wang, L. M. Liu, X. W. Lou, A sulfur host based on titanium monoxide@carbon hollow spheres for advanced lithium–sulfur batteries.Nat. Commun. 7 ,13065(2016)

[28] S.Evers,T.Yim,L.F.Nazar,Understanding the nature of absorption/adsorption in nanoporous polysulfide sorbents for the Li–S battery, J. Phys. Chem. C .116,19653–19658(2012)

[29] B.Cao, Y.Chen, D.Li, L.Yin, Y.Mo,Synthesis of TiC Nanoparticles Anchored on Hollow Carbon Nanospheres for Enhanced Polysulfide Adsorption in Li-S Batteries. *ChemSusChem*. 9,3338-3344(2016)

[30] Z.Li, Y.Huang, L.Yuan, Z.Hao,Y .Huang ,Status and prospects in sulfur-carbon composites as cathode materials for rechargeable lithium-sulfur batteries, Carbon 92 ,41–63(2015)

[31] Liang, Z.H.Sun ,F .Li,H.M.Cheng,Carbon materials for Li–S batteries: functional evolution and performance improvement, Energy Storage Mater. 2 ,76–106(2016)

[32] He, Y.Chen, P.Li, F.Fu , Z.Wang, W.Zhang, Three-dimensional CNT/graphene sulfur hybrid sponges with high sulfur loading as superior-capacity cathodes for lithium–sulfur batteries, J. Mater. Chem. A 3,18605–18610(2015)

[33]Z.S.Li ,S.Ji, G. Pollet Bruno,P.K.Shen,A Co_3W_3C promoted Pd catalyst exhibiting competitive performance over Pt/C catalysts towards the oxygen reduction reaction.*Chem Commun.* 50,566-568(2014)

[33] J.Yan, X.Liu, M.Yao, X.Wang, T.K.Wafle, B.Li ,Long-life, high-efficiency lithium sulfur battery from a nanoassembled cathode, Chem. Mater. 27, 5080–5087(2015)

[34] C.Y.He, J.Z.Tao,Two-dimensional Co_3W_3C nanosheets on graphene nanocomposition: An Pt-like electrocatalyst toward hydrogen evolution reaction in wide pH range. Nano Energy 8,65-72(2018)

[35] P.F.Zhao, Z.Zhang,H.X.He, Y.H.Yu , X.Lia, W.C.Xie , Z.Y.Yang , J.X.Cai ,Cobalt-Tungsten Bimetallic Carbide Nanoparticles as Efficient Catalytic Material for High-Performance Lithium–Sulfur Batteries.*ChemSusChem* 12,4866-4873(2019)

[36] J. He, Y. Chen, P. Li, F. Fu, Z. Wang, W. Zhang, Three-dimensional CNT/graphene sulfur hybrid sponges with high sulfur loading as superior-capacity cathodes for lithium–sulfur batteries, J. Mater.

Chem. A 3 , 18605–18610 (2015)

[37] S.Liang, C.Liang, Y.Xia, H.Xu, H.Huang, X.Tao, Y.Gan,W.Zhang,Facile synthesis of porous Li_2S@C composites as cathode materials for lithium-sulfur batteries, J. Power Sources 306 ,200–207(2016)

[38] T.Sun, Q.Wu, R.Che, Y.Bu, Y.Jiang, Y .Li, L.Yang, X.Wang, Z.Hu, Alloyed Co–Mo nitride as high-performance electrocatalyst for oxygen reduction in acidic medium, ACS Catal. 5,1857–1862(2015)

[39]Q.Yang.M, D.F.Deng, J.Z.Li,L.Y.Chen ,S.D.Guo, J.Liu , H.Chen, Fabrication and mechanical properties of WC-10Co cemented carbides with plate-like WC grains.J.Alloy. Comp.803,860-865(2019)

[40] K.Lee, A. Ishihara, S.Mitsushima, N.Kamiya, KI.Ota,Catalytic activity of titanium oxide for oxygen reduction reaction as a non-platinum catalyst for PEFC.Electrochim. Acta. 49,3479-3485(2004)

[41]F. Li , Q.H.Liu, J.W.Hu, Y.Z.Feng , P.B.He, J.M.Ma, Recent advances in cathode materials for rechargeable lithium-sulfur batteries, Nanoscale 11,15418–15439(2019)

[42]H.J. Peng,G. Zhang,X. Chen,Z.W. Zhang,W.T. Xu,J.Q. Huang,Q .Zhang,Enhanced electrochemical kinetics on conductive polar mediators for lithiumsulfur batteries. Angew. Chem. Int. Edit. 55, 12990–12995(2016)

[43]D.G.Xiong , Z.Zhang, X.Y.Huang, Y.Huang, J.Yu, J.X.Cai, Z.Y.Yang,Boosting the polysulfide confinement in B/N-codoped hierarchically porous carbon nanosheets via Lewis acid-base interaction for stable Li-S batteries.J. Energy Chem 51,90–100(2020)

[44] H.Chen, C.Wang, W.Dong, W. Lu, Z.Du ,L.Chen,Monodispersed sulfur nanoparticles for lithium-sulfur batteries with theoretical performance, Nano Lett. 15,798–802 (2014)

[45] Z.Zhang, A.H.Shao, D.G.Xiong, J.Yu, N.Koratkar, Z.Y.Yang, Facile synthesis of a “two-in-one” sulfur host featuring metallic-cobalt-embedded N-doped carbon nanotubes for efficient lithium-sulfur batteries.ACS Appl. Mater. Interfaces 2,19572–19580(2020)

[46] Z. Lin, C. Liang,Lithium-sulfur batteries: from liquid to solid cells. J. Mater. Chem. A 3,936-958(2015)

[47] J.Sun, Y.Sun, M.Pasta , G.Zhou, Y.Li,W. Liu , F.Xiong, Y.Cui ,Entrapment of polysulfides by a black-phosphorus-modified separator for lithium-sulfur batteries. Adv. Mater 28,9797–9803(2016)

[48]] J.Pu, Z.Shen , J.Zheng , W. Wu, C.Zhu, Q.Zhou, H.Zhang, F.Pan ,Multifunctional Co_3S_4@sulfur nanotubes for enhanced lithium-sulfur battery performance, Nano Energy. 37, 7–14(2017)

[49] M.Zhu, C .Tan,Q .Fang , L.Gao, G.Sui, X.Yang,High performance and biodegradable skeleton material based on soy protein isolate for gel polymer electrolyte.ACS Sustain. Chem. Eng 4 ,4498–4505(2016)

[50]Z.Yuan , H.J.Peng, T.Z.Hou, J.Q.Huang, C.M.Chen , D.W.Wang, X.B.Cheng, F.Wei, Q.Zhang, Powering lithium-sulfur battery performance by propelling polysulfide redox at sulfiphilic hosts .Nano Lett .16,519–527(2016)

Figures

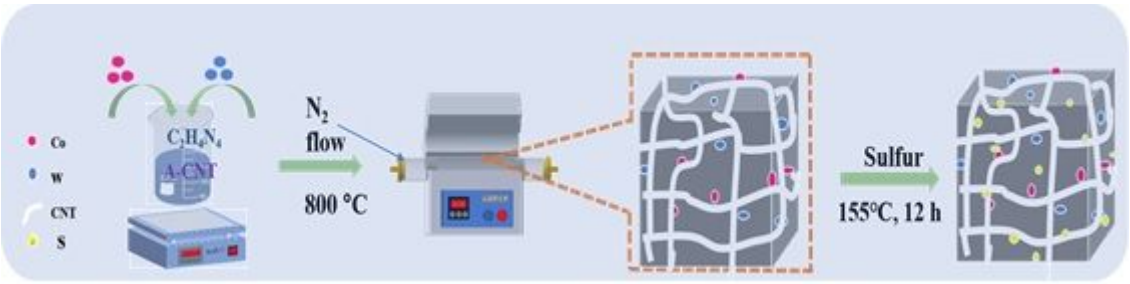

Figure 1

Preparation process diagram of the Co3W3C@C@CNTs/S

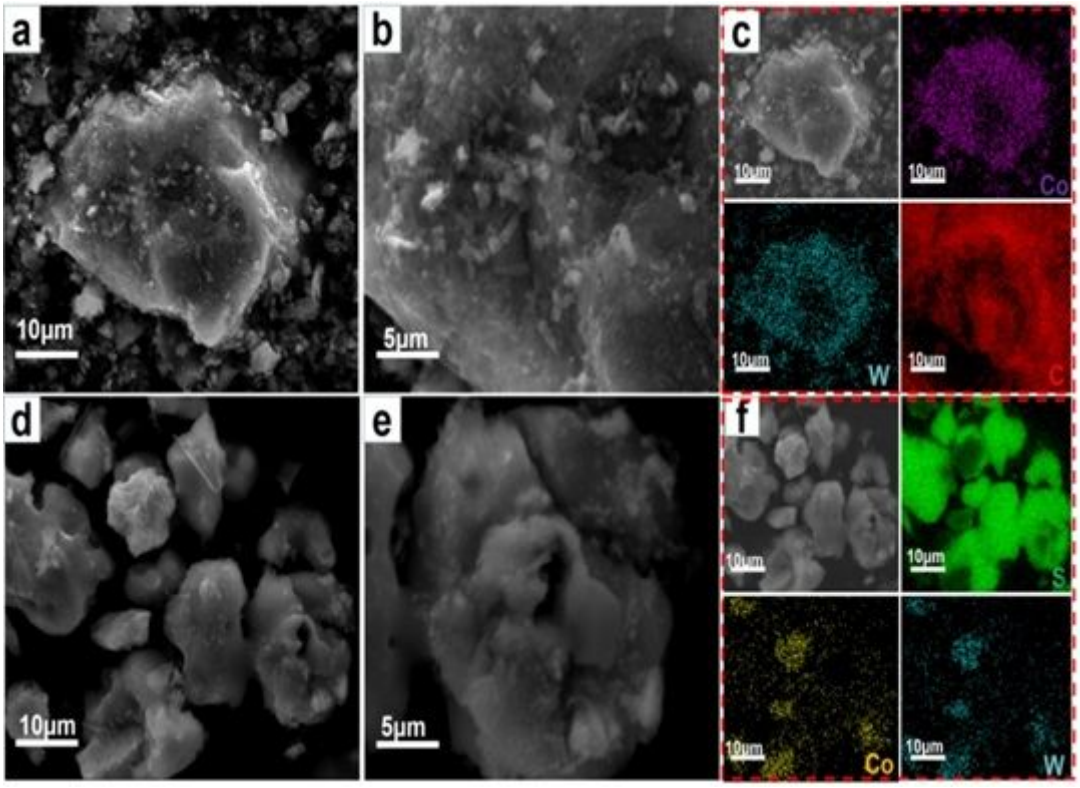

Figure 2

(a–c) SEM images and elemental mapping of the Co3W3C@C@CNTs; and (d–f) SEM images and elemental mapping of Co3W3C@C@CNTs/S

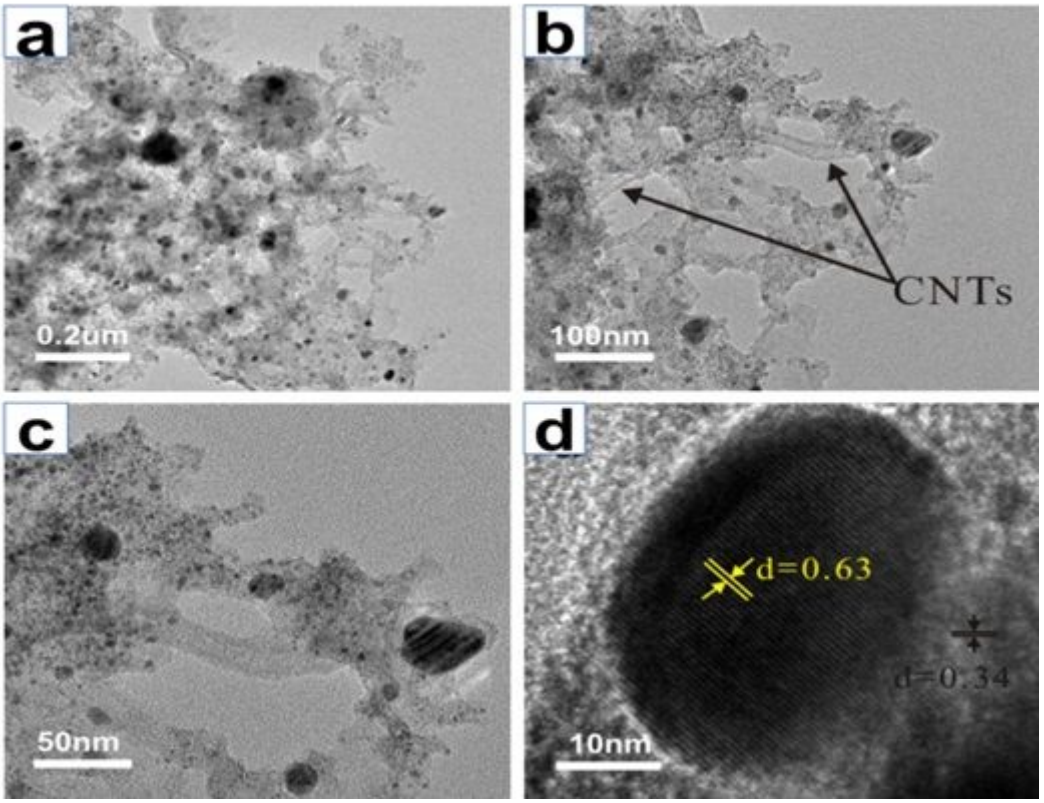

Figure 3

(a-c)TEM and HRTEM diagram of Co3W3C@C@CNT composites.

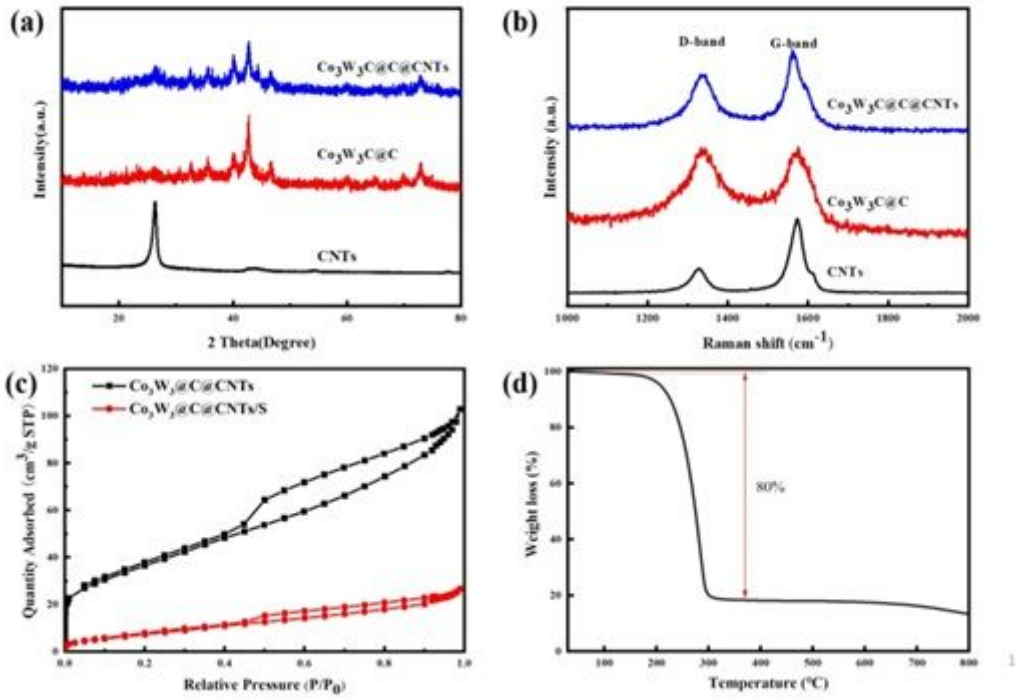

Figure 4

(a) XRD pattern of the CNTs、Co3W3C@C and Co3W3C@C@CNTs; (b) Raman spectra of CNT, Co3W3C@C, and Co3W3C@C@CNT composites; (c) nitrogen adsorption–desorption isotherms of Co3W3C@C@CNTs、Co3W3C@C@CNTs/S; and (d)TGA analysis of Co3W3C@C@CNTs/S

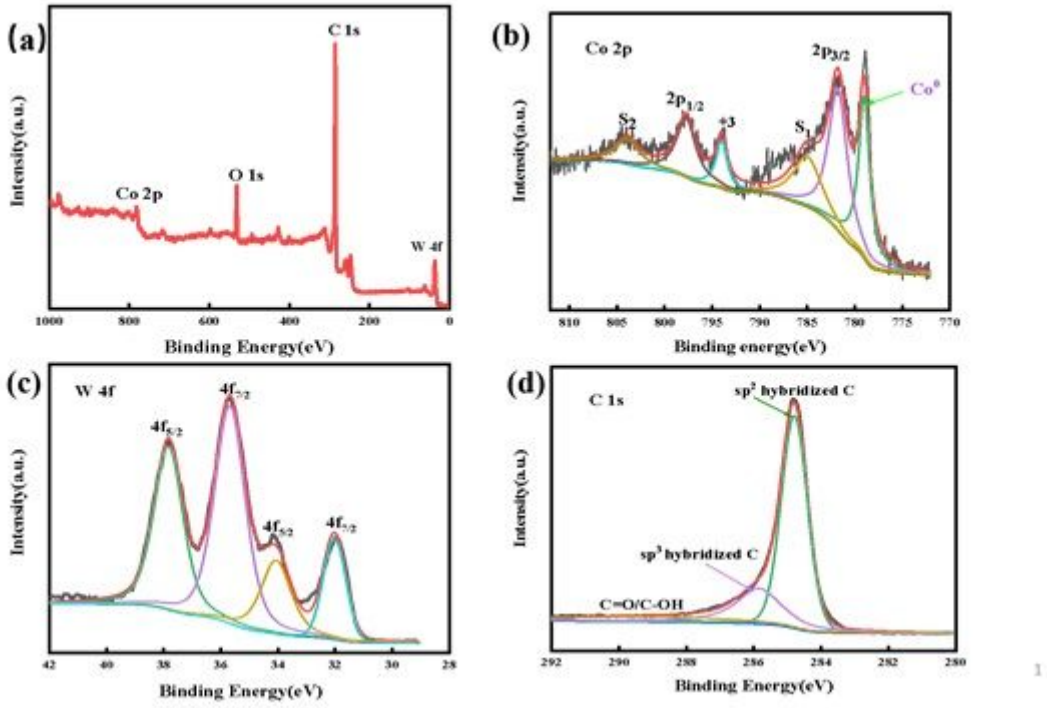

Figure 5

(a) XPS spectra of Co3W3C@C@CNTs, and (b) Co 2p (c) W 4f and(d) C 1s

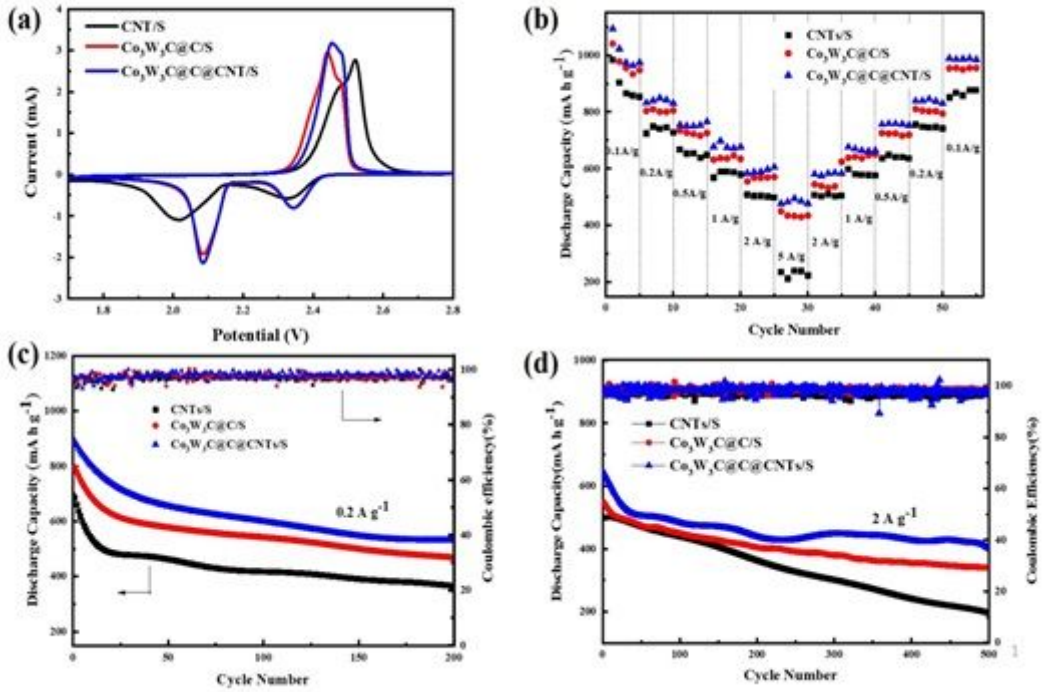

Figure 6

(a) CV curves of CNTs/S, Co3W3C@C/S, and Co3W3C@C@CNTs/S at 0.1 mVs−1; (b) Rate performance of CNTs/S, Co3W3C@C/S, and Co3W3C@C@CNTs/S at different current densities; and the (c–d) cycle performance and Coulombic efficiency of CNTs/S, Co3W3C@c/S, and Co3W3C@C@CNTs/S at 0.2 and 2 A g-1

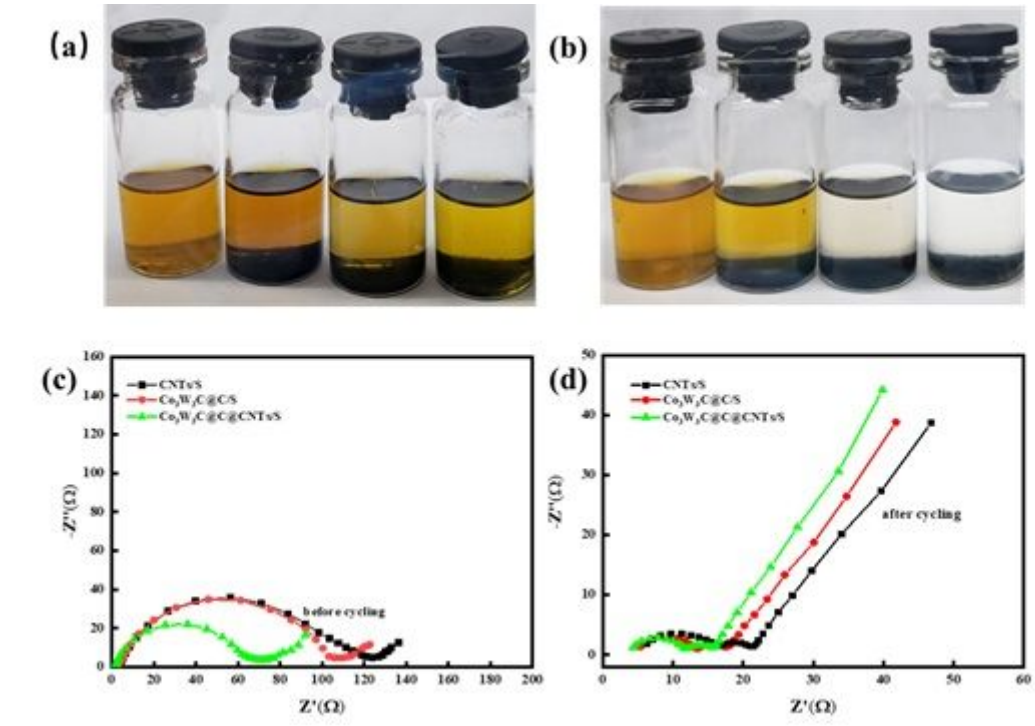

Figure 7

(a) Optical photos of Li2S8 solution before and (b)_after adding blank, CNTs, Co3W3C@C, and Co3W3C@C@CNTs (after 6 h); and (c) EIS profiles of the CNTs/S, Co3W3C@C/S, and Co3W3C@C@CNTs/S electrodes before cycling and (d) after 500 cycles at 2 A g-1.

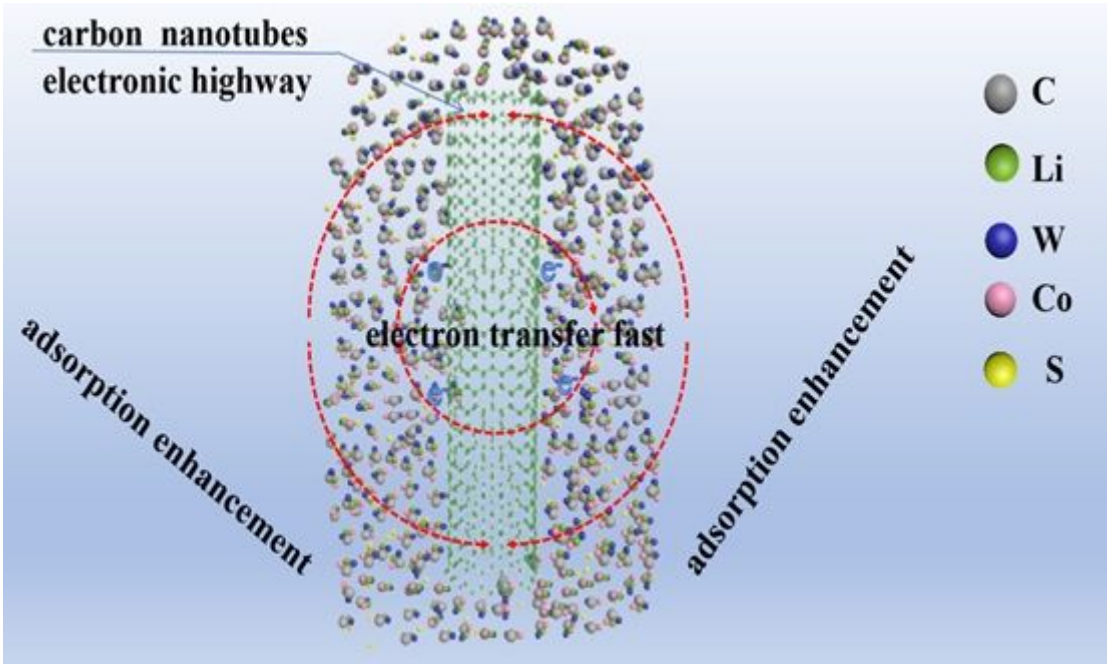

Figure 8

Schematic diagram of Co3W3C@C@CNTs/S